Journal of Neurology (2019) 266:2718–2733
https://doi.org/10.1007/s00415-019-09473-z

ORIGINAL COMMUNICATION

The clinical and radiological profile of primary lateral sclerosis: a population-based study

Eoin Finegan[1] · Rangariroyashe H. Chipika[1] · Stacey Li Hi Shing[1] · Mark A. Doherty[2] · Jennifer C. Hengeveld[2] · Alice Vajda[2] · Colette Donaghy[3] · Russell L. McLaughlin[2] · Niall Pender[1,4] · Orla Hardiman[1] · Peter Bede[1]

Received: 2 July 2019 / Revised: 9 July 2019 / Accepted: 11 July 2019 / Published online: 19 July 2019

Abstract

Background Primary lateral sclerosis is a progressive upper-motor-neuron disorder associated with markedly longer survival than ALS. In contrast to ALS, the genetic susceptibility, histopathological profile and imaging signature of PLS are poorly characterised. Suspected PLS patients often face considerable diagnostic delay and prognostic uncertainty.

Objective To characterise the distinguishing clinical, genetic and imaging features of PLS in contrast to ALS and healthy controls.

Methods A prospective population-based study was conducted with 49 PLS patients, 100 ALS patients and 100 healthy controls using genetic profiling, standardised clinical assessments and neuroimaging. Whole-brain and region-of-interest analyses were undertaken to evaluate patterns of grey and white matter degeneration.

Results In PLS, disease burden in the motor cortex is more medial than in ALS consistent with its lower limb symptom-predominance. PLS is associated with considerable cerebellar white and grey matter degeneration and the extra-motor profile of PLS includes marked insular, inferior frontal and left pars opercularis pathology. Contrary to ALS, PLS spares the postcentral gyrus. The body and splenium of the corpus callosum are preferentially affected in PLS, in contrast to the genu involvement observed in ALS. Clinical measures show anatomically meaningful correlations with imaging metrics in a somatotopic distribution. PLS patients tested negative for *C9orf72* repeat expansions, known ALS and HSP-associated genes.

Conclusions Multiparametric imaging in PLS highlights disease-specific motor and extra-motor involvement distinct from ALS. In a condition where limited post-mortem data are available, imaging offers invaluable pathological insights. Anatomical correlations with clinical metrics confirm the biomarker potential of quantitative neuroimaging in PLS.

Keywords Primary lateral sclerosis · Amyotrophic lateral sclerosis · Neuroimaging · MRI · Genetics

Abbreviations

AD	Axial diffusivity
ALS	Amyotrophic lateral sclerosis
C9orf72	Chromosome 9 open reading frame 72
CST	Corticospinal tract
DTI	Diffusion tensor imaging
EPI	Echo-planar imaging
FA	Fractional anisotropy
FDR	False discovery rate
FTD	Frontotemporal dementia
FOV	Field-of-view
FWE	Familywise error
GM	Grey matter
HARDI	High angular resolution diffusion imaging
HC	Healthy control
HSP	Hereditary spastic paraplegia
LMN	Lower motor neuron
MD	Mean diffusivity
MND	Motor neuron disease
MR	Magnetic resonance
PMC	Primary motor cortex
QBI	q-Ball imaging
RE	Repeat expansion

✉ Peter Bede
bedep@tcd.ie

[1] Computational Neuroimaging Group, TBSI, Trinity College Dublin, Dublin, Ireland

[2] Complex Trait Genomics Laboratory, Smurfit Institute of Genetics, Trinity College Dublin, Dublin, Ireland

[3] Western Health and Social Care Trust (WHSCT), Northern Ireland, UK

[4] Department of Psychology, Beaumont Hospital, Dublin, Ireland

RD	Radial diffusivity
SC	Spinal cord
TBSS	Tract-based spatial statistics
TE	Echo time
TFCE	Threshold-free cluster enhancement
TR	Repetition time
UMN	Upper motor neuron
VBM	Voxel-based morphometry
WM	White matter

Introduction

Primary lateral sclerosis (PLS) is an uncommon neurodegenerative motor neuron disease of unknown aetiology [1]. The clinical profile of PLS entails progressive symmetric spinobulbar spasticity in the absence of muscle atrophy [2]. The distinction between PLS and ALS is not merely of academic interest, as PLS is associated with markedly longer survival [3]. As ALS patients may initially present with UMN-predominant symptoms, current diagnostic criteria for PLS require a period of 4 years with isolated upper motor neuron involvement and the absence of LMN signs [4]. This long observation period typically coincides with a phase of significant functional decline in PLS [5]. Beyond the psychological burden of diagnostic uncertainty, this is potentially a valuable period for neuroprotective intervention and enrolment to clinical trials. Currently, suspected PLS patients are excluded from ALS trials and even once diagnostic criteria are met, very few PLS-specific trials are conducted [6].

While PLS imaging studies often suffer from considerable sample size limitations [6], they invariably demonstrate significant corticospinal tract [7, 8], corpus callosum [9, 10], and precentral gyrus atrophy [11, 12] similar to the imaging signature of ALS. PLS imaging studies often include ALS cohorts [13], but symptom duration differences are seldom accounted for [14]. With few exceptions [15], the majority of PLS studies describe overlapping anatomical patterns of pathology in ALS and PLS without identifying distinguishing features [8, 16]. Disease burden distribution within the motor cortex, segmental corpus callosum vulnerability, and somatotopic correlations with motor disability have not been characterised in PLS to date [17]. As the diagnosis of PLS requires 4-year symptom duration, the reliable identification of distinguishing imaging characteristics between PLS and ALS would require robust corrections for symptom duration, rigorous adjustments for demographic factors [18], and targeted region-of-interest analyses. Furthermore, PLS imaging studies are strikingly inconsistent regarding extra-motor and cerebellar involvement [19–23]. The relevance of large, single-centre prospective PLS studies is not merely academic, they may capture distinguishing imaging features between ALS and PLS and lead to the identification of early PLS-associated changes before current diagnostic criteria are met [15]. Accurate diagnostic biomarkers in PLS would not only reduce diagnostic uncertainty but would enable early patient stratification in clinical trials [24]. The establishment and validation of PLS-specific imaging signatures may also help to assess the risk of conversion to ALS in suspected cases. Moreover, exceptionally few autopsy reports are available in PLS and systematic comparisons with ALS cases are lacking [25, 26]. Accordingly, the objective of this study is the comprehensive and comparative characterisation of PLS-associated pathology in vivo. Additional objectives include the evaluation of extra-motor and cerebellar involvement in PLS, assessment of focal motor cortex alterations, correlations with motor disability, and comprehensive genetic, clinical and cognitive profiling.

Our hypothesis is that distinguishing imaging traits can be identified between ALS and PLS using a dedicated imaging protocol. Given the lack of lower motor neuron involvement in PLS, we hypothesise that focal somatotopic clinico-cortical correlations can be captured.

Methods

Participants

Forty-nine patients with PLS, 100 patients with ALS and 100 healthy controls (HC) were included in a prospective clinical, genetic and multiparametric neuroimaging study (Fig. 1). The study was approved by the Ethics (Medical Research) Committee—Beaumont Hospital, Dublin, Ireland, and all participants provided informed consent prior to inclusion. Participating ALS patients had 'probable' or 'definite' ALS according to the El Escorial criteria [27] and PLS patients were diagnosed according to the Gordon criteria [4]. Inclusion criteria in the imaging component of the study included the ability to lie supine in the scanner for the duration of data acquisition. The healthy control cohort had no known neurological or psychiatric conditions, previous head injuries or established vascular risk factors.

Clinical assessments

PLS patients underwent standardised clinical evaluation including the Penn UMN burden score which provides a composite score of pathologically-increased reflexes for each limb and bulbar region, and limb spasticity measured on the modified-Ashworth scale [28, 29]. Finger-tapping (index finger-to-thumb) and foot-tapping rates were recorded over 20 s, with three repetitions for each limb. The best performance was used to calculate tapping-rate. Cognition was evaluated using the Edinburgh Cognitive ALS

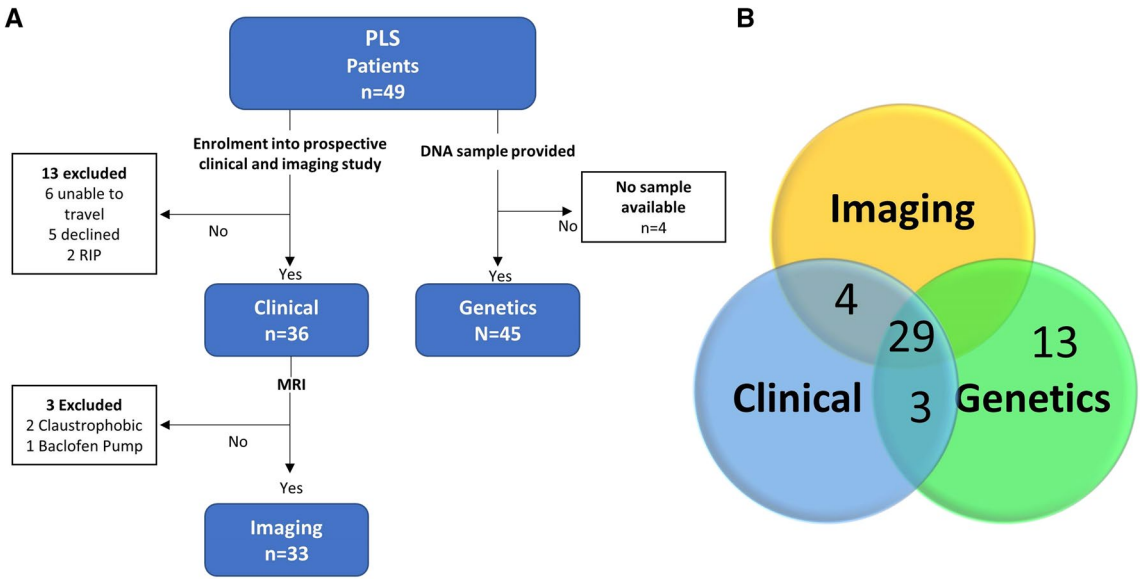

Fig. 1 **a** Flow diagram of patient recruitment and participation in the imaging, clinical and genetic aspects of the study. Reasons for exclusion are shown where applicable. **b** Venn diagram highlighting the overlapping participation of PLS patients in one, two or all three components of the research study

Screen (ECAS). This instrument has been validated in an Irish cohort and age and education-based normative values are available to detect impairments in language, verbal fluency, executive, memory and visuospatial domains [30]. The revised ALS functional rating scale (ALSFRS-r) was used to establish the severity and pattern of functional disability in the PLS and ALS groups [31].

Genetic testing

Exome sequencing was performed for 45 PLS patients (Fig. 1) to a mean target coverage of 35× on an Illumina NovaSeq with 2 × 150 bp sequencing. Sequence data were assessed for quality, aligned to the GRCh37 reference genome and variants were called, annotated and analysed using cutadapt V.1.9.1 [32], SAMtools V1.7 [33], Picard V.2.15.0 (https://picard.sourceforge.net/), Plink V.1.9 [34], R V.3.2.3 (https://www.r-project.org/), SnpEff V.4.3 [35] and Gemini V.0.20.1 [36]. Samples were compared to 135 Irish controls sequenced as described previously [37]. One sample failed quality control. Putative variants were defined as protein altering variants in the exons and splice sites of 33 genes linked to ALS on the ALS online database [38] and 70 genes linked to HSP in the literature [39]. Samples were screened for heterozygous variants absent in controls and with a minor allele frequency (MAF) below 0.01 in population reference datasets [40, 41] or homozygous variants with a MAF below 0.05 in controls or reference datasets. Putative variants were cross-referenced with the Human Gene Mutation Database [42] and an internal literature review to identify variants previously linked to ALS or HSP. The presence of the *C9orf72* hexanucleotide repeat expansion was determined using repeat-primed polymerase chain reaction (PCR) as described previously [43]. CAG repeats in *ATXN2* were detected by PCR in 35 PLS patients and compared with 1011 ALS patients and 593 controls. Intermediate length repeats (24–34 repeats) in ATXN2 are associated with ALS risk and expanded repeats (> 40) cause spinocerebellar ataxia 2 (SCA2). Of the 100 ALS patients enrolled in neuroimaging, whole-genome sequence data was available for 44 patients [37] and targeted DNA sequence data for a further 27 [44]. Patients were screened for previously reported ALS variants. *C9orf72* repeat expansion status was determined in 97 patients.

Neuroimaging methods

Magnetic Resonance (MR) data were acquired on a 3 Tesla Philips Achieva system using an 8-channel receive-only head coil. T_1-weighted images were acquired using a 3D Inversion Recovery prepared Spoiled Gradient Recalled echo (IR-SPGR) sequence, with a field-of-view (FOV) of 256 × 256 × 160 mm, spatial resolution of 1 mm^3, TR/TE = 8.5/3.9 ms, TI = 1060 ms, flip angle = 8°, SENSE factor = 1.5, and an acquisition time of 7 min 30 s. DTI images were acquired using a spin-echo echo planar imaging (SE-EPI) sequence with a 32-direction Stejskal-Tanner diffusion encoding scheme. FOV = 245 × 245 × 150 mm, spatial resolution = 2.5 mm^3, 60 slices were acquired with no interslice gap, TR/TE = 7639/59 ms, SENSE factor = 2.5, *b* values = 0,

1100 s/mm^2, with SPIR fat suppression, dynamic stabilisation and a total acquisition time of 5 min 41 s. A dual approach was undertaken to evaluate anatomical patterns of pathology in PLS. First, standard whole brain analyses were performed to assess grey and white matter alterations. Subsequently, additional region-of-interest (ROI) analyses were undertaken to assess the integrity of specific anatomical regions. Following whole-brain and region-of-interest analyses, anatomical correlations were explored with clinical measures.

Whole-brain imaging analyses

Grey matter pathology in PLS was evaluated by voxel-based morphometry (VBM) and cortical thickness analyses. VBM analyses were carried out using the FMRIB's FSL suite [45, 46]. Standard pre-processing steps were used, including skull-removal (BET), motion-corrections and tissue-type segmentation. Grey-matter partial volume data were aligned to the MNI152 standard space using affine registration. Subsequently, a study-specific GM template was created to which the grey matter images from each subject were non-linearly co-registered. For group comparisons, permutation based non-parametric inference was used with the threshold-free cluster enhancement (TFCE) method. Comparisons of patient groups and controls were corrected for age and gender and the comparison of the ALS and PLS cohorts was additionally corrected for symptom duration. The FreeSurfer image analysis suite was used for cortical thickness measurements [47]. Pre-processing included the removal of non-brain tissue, segmentation of the subcortical white matter and deep grey matter structures, intensity normalization, tessellation of the grey matter-white matter boundary, and automated topology correction [48]. Study groups were first compared at a "whole brain" level using FreeSurfer's Query, Design, Estimate, Contrast (QDEC) application. A general linear model (GLM) was used with age and gender as covariates and False Discovery Rate (FDR) corrections applied.

Region of interest analyses

To illustrate the unique distribution profile of grey matter pathology in ALS and PLS in the motor cortex, additional morphometric analyses were carried out restricting the analyses to the precentral gyrus. The precentral gyrus label of the Harvard–Oxford probability atlas [49] and the design matrices including group membership, age and gender were used for ROI morphometry. PLS-specific, ALS-specific and overlapping grey matter involvement in the precentral gyrus was visualised with respect to controls at $p < 0.01$ TFCE FWE. Supplementary region-of-interest cortical thickness analyses were carried out on cortical measures from atlas-defined regions. The Desikan–Killiany Atlas was used to define the following cortical regions in each hemisphere; precentral gyrus, paracentral gyrus, post-central gyrus, left pars triangularis and left pars opercularis regions. Average cortical thickness values were retrieved from the above regions and boxplots of raw values were generated to highlight differences between the study groups. Subsequently, assumptions of normality, linearity and homogeneity of variances were verified and analyses of covariance (ANCOVAs) were performed with ROI values included as dependent variables, study group membership (PLS, ALS or HC) as the independent variable. A p value of < 0.05 was considered significant. Results are summarised in Table 2, including the estimated marginal means of ROI values, standard error, between-group ANCOVA significance and post hoc group comparisons. The comparisons of PLS and ALS cohorts were corrected for symptom duration in addition to age and gender.

White matter analyses

Following eddy current corrections and skull removal a tensor model was fitted to the raw diffusion data to generate maps of fractional anisotropy (FA), axial diffusivity (AD), and radial diffusivity (RD). The tract-based statistics (TBSS) pipeline of the FSL image analysis suite was utilised for non-linear registration and skeletonisation of each subject's images. FA, AD and RD images were merged into a single 4D image file and a mean FA mask was created. Similarly to the VBM analyses, permutation-based non-parametric inference was used for the voxelwise comparison of diffusivity parameters between PLS and ALS using design matrix-defined contrasts which included age, gender and symptom duration as covariates. Comparisons between PLS and healthy controls were adjusted for age and gender. The threshold-free cluster enhancement (TFCE) method was applied and results considered significant at a $p < 0.05$ TFCE family-wise error (FWE). Following standard tract-based spatial statistics, supplementary ROI white matter analyses were also carried out. The study specific white matter skeleton was masked by atlas-defined labels for the corticospinal tracts, body of the corpus callosum, forceps minor (genu), forceps major (splenium) and cerebellum to generate study specific ROIs. The MNI atlas was used to define the cerebellar hemispheres and the labels of the Jülich histological atlas [50] was used to define the CST and segments of the corpus callosum. Diffusivity metrics; axial diffusivity, fractional anisotropy and radial diffusivity were retrieved from the above ROIs and study group differences were evaluated in analyses of covariance, accounting for age, gender and in the PLS versus ALS contrast also for symptom duration. For illustrative purposes raw values from individual subjects were also plotted in boxplots. The imaging correlates of basic clinical measures were explored

using permutation-based non-parametric statistics on skeletonised FA data in FSL. The following clinical measures were included in 'whole-brain' tract-based analyses; bulbar ALSFRS-r subscores, lower limb ALSFRS-r subscores, upper limb ALSFRS-r subscores and tapping rates in the four limbs. Clinical measures were demeaned and incorporated in design matrices including age, gender and symptom duration as covariates. The resulting statistical maps were thresholded at $p < 0.05$ FWE TFCE.

Results

Clinical characteristics

The demographic profile of study participants is summarised in Table 1. Standardised clinical assessments were performed on 36 of the 49 PLS (73%) subjects (Fig. 1). The mean age of this subgroup was 62.1 years (SD 10.8). The mean age of symptom onset was 51.5 years (SD 8.7) and the mean symptom duration was 120.8 months (SD 20.6).

Site of symptom onset was in the lower limbs in 35 of 36 (97%) PLS patients assessed. Only one patient presented with dysarthria and signs of pseudobulbar palsy prior to the development of lower limb symptoms. No PLS patient experienced their initial symptom in the upper limbs, although at the time of study evaluation, 94% had functional upper limb impairment. All 36 individuals had clinical signs of UMN dysfunction in the upper limbs. Most PLS patients (91%) required some form of walking aid and 78% had experienced at least one fall during the preceding 12-months. The comparison of lower and upper limb disability based on ALSFRS-r sub-scores indicated that lower limb function ($M = 5.39$, SD 1.57) was significantly more affected than upper limb function ($M = 8.64$, SD 2.00); $p < 0.001$. No individual within the PLS group had a lower upper limb sub-score than their lower limb ALSFRS sub-score, highlighting striking clinical homogeneity in regional involvement. Pseudobulbar motor impairment was reported in 78%, as indicated by ALSFRS-r bulbar sub-scores ($M = 9.19$, SD 2.18), while pseudobulbar UMN signs (jaw-jerk, pout/facial, palmomental reflex) were detected in 80%. Individually these signs were present in 50%, 50% and 34% of patients, respectively. None of the PLS patients required gastrostomy and respiratory function was well-preserved across the group ($M = 11.14$, SD 1.33). Neurological examination demonstrated widespread spasticity and pathologically increased reflexes, without significant weakness in all PLS patients. A markedly symmetrical pattern of spasticity was observed with no significant within-subjects difference between the left and right spasticity scores; $p = 0.10$. Consistent with the observed lower-limb symptom predominance, spasticity was significantly greater in the lower limbs (Mean = 3.53, SD 0.77) than in the upper limbs (Mean = 2.88, SD 0.97); $p < 0.001$. UMN-burden limb sub-scores negatively correlated with finger tapping rates in the upper limbs (Right upper limb $r = -0.67$, $n = 32$ $p < 0.001$; Left upper limb $r = -0.66$, $n = 32$, $p < 0.001$). A significant association was also identified between left lower limb UMN-burden sub-scores and left foot-tapping rates ($r = -0.44$, $n = 31$, $p = 0.013$). A similar trend was also observed between UMN-burden and tapping rates in the right lower limb ($r = -0.32$, $n = 31$, $p = 0.075$). Lower foot-tapping rates were associated with reduced lower limb functional scores; ($r = 0.57$, $n = 31$, $p = 0.001$) and lower finger-tapping rates correlated with reduced upper limb functional sub-scores ($r = 0.44$, $n = 33$, $p = 0.001$). Cognitive impairment was detected in at least one domain of the ECAS in 36% of the

Table 1 (A) The demographic profile of all study participants. (B) The demographic and clinical profiles of PLS subjects participating in both standardised imaging and clinical assessments, in comparison with ALS subjects and healthy control (HC) group

(A) All study participants				
	PLS $n = 49$	ALS $n = 100$	HC $n = 100$	p value
Gender (male (%))	29 (59%)	61 (61%)	48 (48%)	0.15
Age—years (mean ± SD)	62.72 ± 10.17	60.73 ± 9.73	58.79 ± 11.53	0.10
(B) Imaging study participants				
	PLS $n = 33$	ALS $n = 100$	HC $n = 100$	p value
Gender (male (%))	19 (57%)	61 (61%)	48 (48%)	0.17
Age—years (mean ± SD)	60.48 ± 10.48	60.73 ± 9.73	58.79 ± 11.53	0.41
Handedness (right (%))	29 (87%)	91 (91%)	89 (89%)	0.83
Education (years)	12.88 ± 3.38	12.8 ± 2.92	13.62 ± 2.78	0.121
ALSFRS-r	34.36 ± 5.33	36.62 ± 7.47	N/A	0.11

PLS cohort. The most commonly observed deficits were in language (22%) and verbal fluency (17%) domains. Memory impairment was present in 11%, while executive impairment (6%) and visuospatial impairment (3%) were less prevalent.

Genetic analysis

The 45 PLS subjects who underwent genetic analysis were demographically representative of the total group of 49; 26 males (58%), mean age of 62.6 years (SD 9.22). All PLS patients tested negative for the *C9orf72* repeat expansions (< 30 repeats). In *ATXN2*, the frequency of intermediate length repeats in PLS patients 2.86% [95% CI 0.35–9.94%] cannot be statistically distinguished from the frequency in controls (2.95% [95% CI 2.00–3.99%]; pPLS-control = 1, Fisher's exact test) or the frequency in ALS cases (4.21% [95% CI 3.38–5.18%]; pPLS-ALS = 1, Fisher's exact test). After filtering, 48 putative single nucleotide variants or indels were identified in 33 HSP or ALS genes. Five of these were previously reported variants (LYST:c.11086G>A[p.V369I]; SPG7:c.1727C>G[S576W]; SQSTM1:c.328C>T[p.R110C]; TAF15:c.1222C>T[p.R408C]; TAF15:c.1163G>A[p.R388H]), however all lacked segregation evidence and statistical support in the literature. Eleven of 97 ALS patients carried the *C9orf72* repeat expansion. Additionally, eight previously reported variants were identified in seven ALS patients (*ALS2*:c2566A>G[p.T856A]; *ALS2*:c.4119A>G[p.I1373M]; *CHMP2B*:c.618A>C[p.Q206H]; *SETX*:c.820A>G[p.M274V]; *SPAST*:c.131C>T[p.S44L]; *SPG11c*.7069C>T[p.L2355F]; *TAF15*:c.1163G>A[p.R388H]; *TARDBP*:c.859G>A[p.G287S]).

Imaging results

Thirty-three PLS subjects, 100 ALS subjects and 100 healthy control subjects underwent standardised neuroimaging (Fig. 1). All imaged patients also completed the standardised clinical assessment on the day of their scan. The demographic and basic clinical details of the imaged sub-group of PLS patients, in comparison with ALS and healthy controls are presented in Table 1B. The imaged sub-group is representative of the total group of clinically-assessed subjects in terms of ALSFRS sub-scores, disability profile, UMN-burden, tapping rates and cognition. The disability profile of imaged patients based on ALSFRS-r sub-scores: bulbar $M = 9.24$, SD 2.14; upper limb $M = 8.61$, SD 2.09; lower limb 5.39, SD 1.62; respiratory $M = 11.12$; SD 1.36.

Grey matter findings

Standard VBM revealed considerable grey matter atrophy in the bilateral insula, right cerebellar hemisphere, left pars opercularis region, left frontal pole, bilateral temporal poles, and the motor cortex in PLS cohort with reference to healthy controls $p < 0.005$ FWE TFCE. Figure 2a. The comparison of ALS and PLS patients revealed more cerebellar, precentral gyrus, thalamic and right dorsolateral prefrontal cortex pathology in PLS than in ALS at $p < 0.05$ TFCE FWE accounting for age, gender and symptom duration. Figure 2b. Cortical thickness and cortical volume analyses in QDEC did not reach significance following FDR corrections over the entire brain.

Tract-based spatial statistics

TBSS detected decreased FA and increased RD in the body of the corpus callosum, cerebellum, and corticospinal tracts in the brainstem, posterior limbs of the internal capsule, corona radiata and centrum semiovale at $p < 0.017$ FWE in PLS compared to healthy controls. At the same statistical threshold axial diffusivity maps only highlighted increased AD in the CST bilaterally. In comparison to ALS patients, the PLS cohort exhibited decreased FA in the body of the corpus callosum and increased cerebellar RD accounting for symptom duration (Fig. 3).

Region of interest analyses (GM and WM)

Region of interest morphometry in the precentral gyrus suggest that PLS-associated pathology is primarily medial, localising to the lower limb representation of the motor cortex, whereas in the ALS cohort the lateral aspect of the PMC is also involved. Figure 2c. Raw values retrieved from grey and white matter ROIs also confirm disease-specific pathological patterns (Fig. 4).

Region of interest grey matter analyses confirmed cortical thinning in the pre- and para-central gyri and left pars opercularis region in the PLS cohort. PLS patients do not exhibit postcentral gyrus atrophy, which differentiates them from the cortical thickness profile of ALS. Statistically significant differences have been detected between the post-central gyrus thickness profiles of the two patient groups bilaterally. (Table 2).

PLS patients exhibit reduced FA and increased RD in the bilateral corticospinal tracts, cerebellar hemispheres, body of corpus callosum and forceps major (splenium) compared to healthy controls. Increased corticospinal tract and cerebellar AD can also be readily detected in PLS compared to controls. Cerebellar FA and RD alterations in PLS are more marked than in PLS even when accounting for differences in symptom duration. The body of the corpus callosum is more affected in PLS than ALS based on regional FA values, but the genu of the corpus callosum is more affected in ALS based on AD. (Table 3).

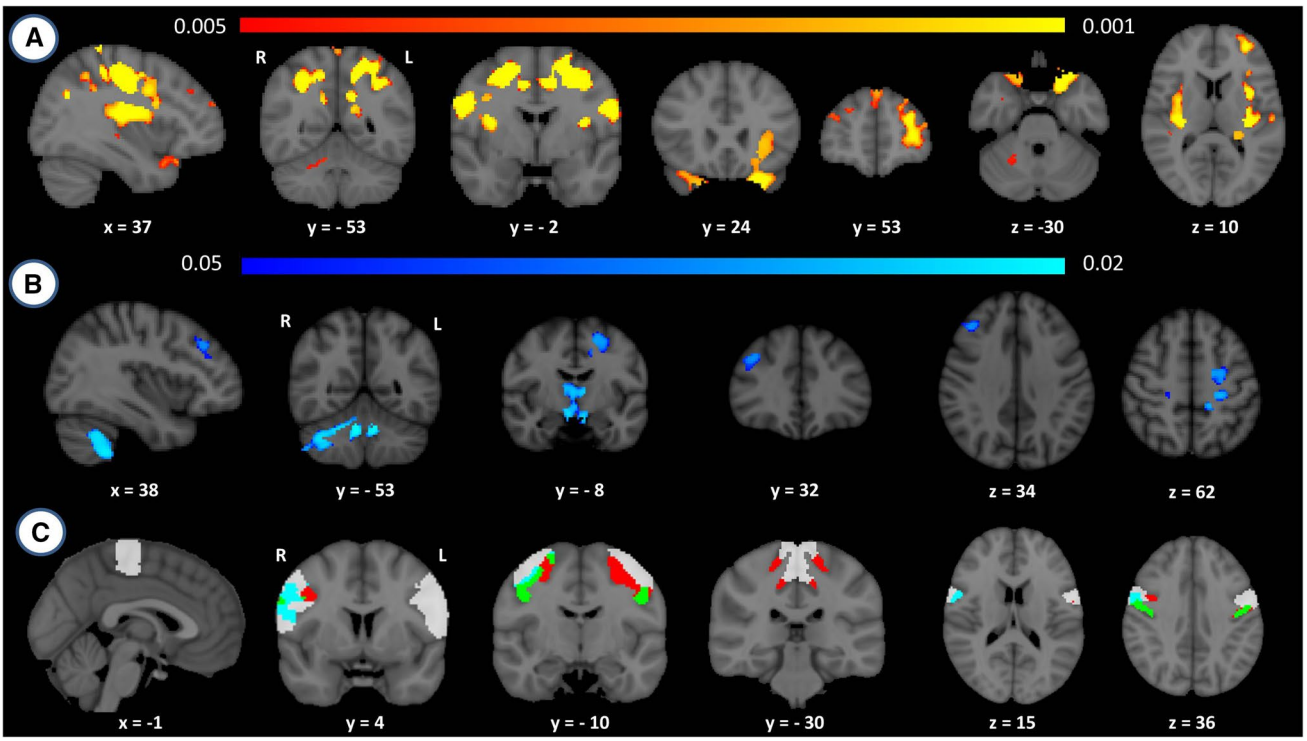

Fig. 2 PLS-associated morphometric changes. **a** Regions of grey matter atrophy in PLS compared to controls at $p < 0.005$ TFCE FWE corrected for age and gender. **b** Comparison of PLS and ALS cohorts. Blue clusters indicate pathology in PLS patients compared to ALS at $p < 0.05$ TFCE FWE corrected for age and gender. **c** Region of interest morphometry restricted to the precentral gyrus (white mask). Blue colour indicates ALS-associated pathology, red colour indicates PLS-associated pathology and green colour the overlap where both ALS and PLS patients exhibit cortical changes in the precentral gyrus with reference to controls at $p < 0.01$ TFCE FWE. Radiological convention is used: *R* right, *L* Left

Correlations

Significant voxelwise anatomical correlations were identified for all three diffusivity metrics in association with ALSFRS-r subscores and tapping rates in a somatotopic distribution. Figure 5. Both tapping rates and ALSFRS-r subscores show correlations within motor tracts subjacent to the somatotopic representation of functional cortical regions in the motor homunculus. Lower limb functional scores and tapping rates correlate with corticospinal fibre integrity subjacent to the medial motor cortex. Upper limb functional scores and tapping rates correlate with FA values under the hand representation of the motor cortex. Clinical correlations with cortical grey matter metrics did not reach statistical significance setting significance at $p < 0.05$ TFCE FWE.

Discussion

Our imaging analyses indicate that PLS has a restrictive imaging signature compared to ALS. PLS exhibits considerable cerebellar, preferential medial motor cortex, and selective corpus callosum involvement with the relative sparing of the postcentral gyrus and genu of the corpus callosum. The lack of lower motor neuron involvement in PLS enables precision clinico-cortical correlations. Our findings also confirm extra-motor involvement in PLS. The distribution of disease burden within the motor cortex is different between PLS and ALS. The marked medial motor cortex atrophy detected on VBM, and the considerable paracentral gyrus thinning on cortical thickness analyses are consistent with the lower limb predominant disability profile of PLS. The somatotopic distribution of motor cortex pathology is also consistent with symptom onset in the lower limbs in the majority of our patients. Contrary to ALS [17], where motor disability is confounded by lower motor neuron degeneration and functional rating scales may be disproportionately influenced by LMN degeneration, PLS is a template condition to observe cerebral somatotopic patterns due to isolated UMN degeneration. This is supported by our whole brain correlation analyses where out of the entire cerebral white matter skeleton strikingly focal and anatomically meaningful correlations were observed in the fibres of the corticospinal tracts subjacent to the functional representations of specific motor functions. Lower limb tapping rates correlate with motor fibre integrity projecting to the medial paracentral

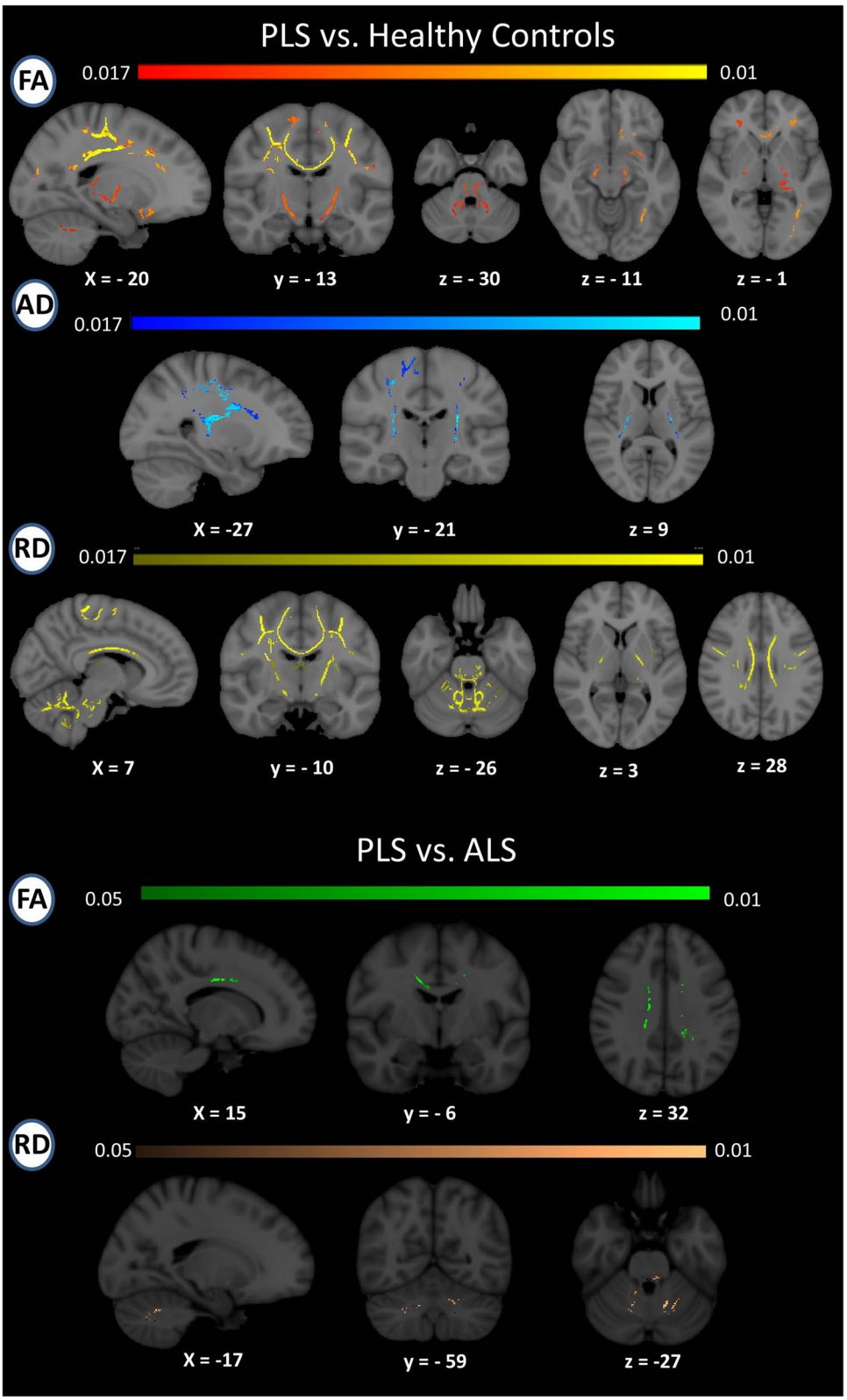

Fig. 3 White matter alterations in PLS in comparison to controls and ALS patients. Top section: Regions of reduced fractional anisotropy (FA) (yellow–red), increased axial diffusivity (AD) (blue) and increased radial diffusivity (AD) (yellow) in contrasts to healthy controls at $p < 0.017$ TFCE FWE corrected for age and gender. Bottom section: regions of decreased FA and increased RD compared to ALS at $p < 0.05$ TFCE FWE corrected for age, gender and symptom duration. Radiological convention is used

sections of the motor homunculus. Upper limb tapping rates correlate better with more lateral projections. Similarly to the imaging correlates of tapping rates, functional subscores also exhibit similar somatotopic correlations. Bulbar subscores in PLS correlate with white matter integrity subjacent to the bulbar representation of the motor homunculus,

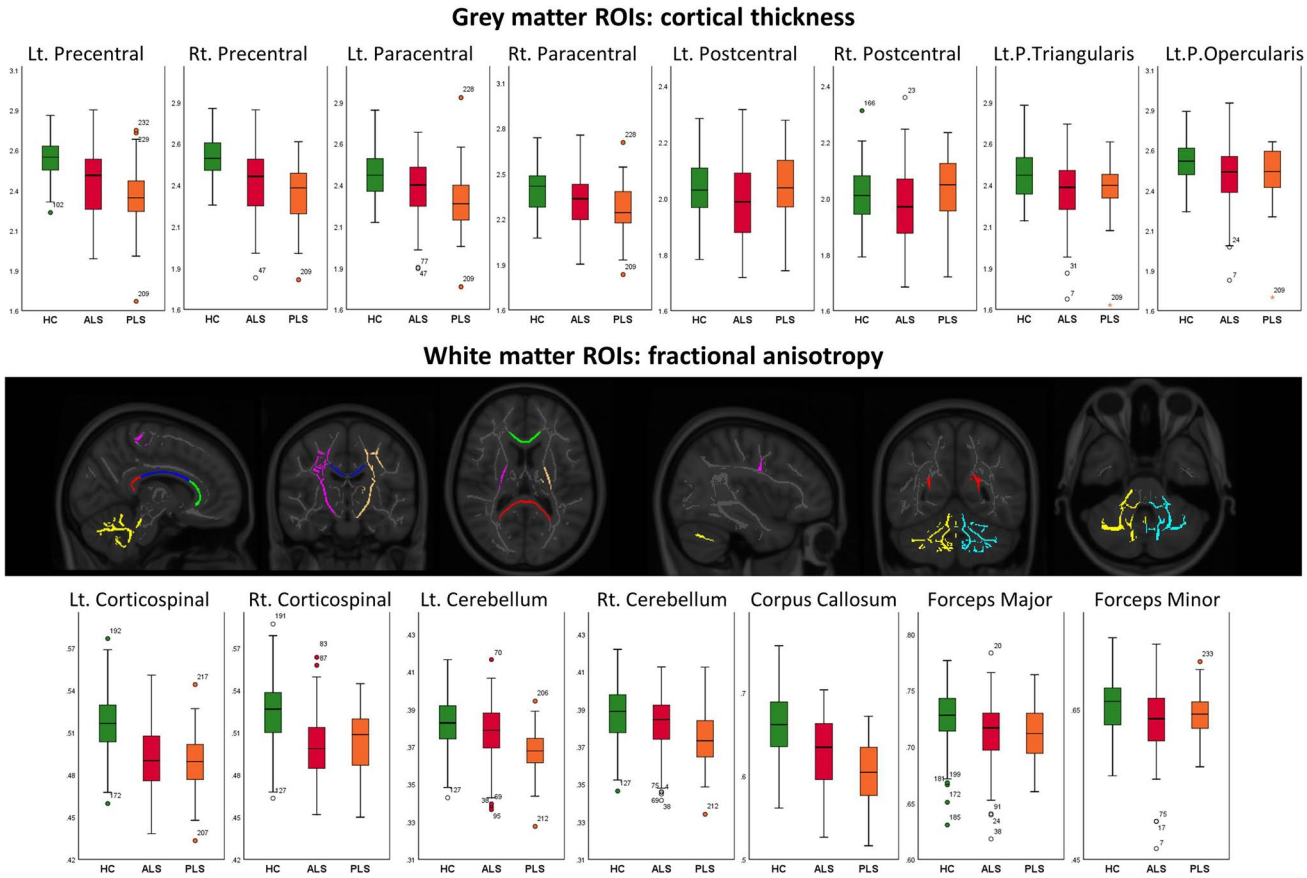

Fig. 4 Box plots of region-of-interest (ROI) grey and white matter measures in the three study groups; healthy controls (green), ALS patients (red), and PLS (orange). Cortical thickness values are provided for grey matter ROIs and fractional anisotropy values are shown as white matter integrity measures. Estimated marginal means adjusted for age and gender, standard error and post hoc *p* values are presented in dedicated tables

lower limb functional scores show medial and upper limb scores more lateral associations. The relevance of sensitive clinico-anatomical correlations is twofold. On the one hand they indicate that simple, cheap clinical measures, such as tapping rates are valid proxies of white matter degeneration in disease-associated regions and may have a role in clinical trials as monitoring markers. On the other hand they confirm that clinical disability in PLS stems from relatively focal pyramidal tract degeneration, which is relatively segmental and predominantly linked to superior CST segments in the corona radiata, as opposed to the preferential pathology seen in the posterior limb of the internal capsule in ALS [51, 52].

The extra-motor clinical profile of PLS is relatively poorly characterised as cerebellar, extrapyramidal behavioural and neuropsychological deficits are rarely studied systematically. Despite sporadic reports [53], a prior study of cognition in PLS found a relatively low prevalence of FTD [54]. The PLS cohort in our study showed neuropsychological deficits particularly in language and verbal fluency domains. Given the strikingly limited post-mortem literature of PLS [6], computational imaging is uniquely positioned to appraise extra-motor involvement in PLS. Our findings indicate bi-insular, pars opercularis and pars triangularis atrophy, and dorsolateral prefrontal cortex pathology. The direct comparison of the ALS and PLS cohorts suggests that cerebellar pathology is an important feature of PLS. Extra-motor white matter pathology is less widespread in PLS and includes cerebellar and occipital white matter areas including the association fibres of the forceps major crossing through the splenium (Fig. 3). At a statistical threshold of $p < 0.017$ TFCE FWE, FA detected the most widespread alterations of any diffusion metric. FA analyses revealed occipital and inferior frontal white matter degeneration in addition to the bi-cerebellar, bilateral corticospinal tract, brainstem and corpus callosum changes which were also detected by AD and RD. Region of interest WM analyses suggest that PLS is primarily associated with white matter changes in the body and splenium of the corpus callosum, whereas ALS also exhibits considerable changes in the association fibres of the forceps minor (Table 3) passing through the genu of the corpus callosum. Not only do different diffusivity parameters have differing detection sensitivities,

Table 2 Regional cortical thickness values in healthy controls (HC), ALS and PLS

Region of interest	Study group	Estimated marginal mean (adjusted for age and gender)	Standard error	ANCOVA Sig. (*p*)	Post-hoc comparisons significant inter-group differences (Bonferroni-corrected)
Regional cortical thickness					
Left precentral gyrus	HC	2.543458	0.016621	1.068E − 12	ALS vs HC $p = 5.6935E-8$*
	ALS	2.405877	0.016595		PLS vs HC $p = 5.7942E-11$*
	PLS	2.308378	0.028775		ALS vs PLS $p = 0.853508$[a]
Right precentral gyrus	HC	2.510695	0.016309	1.4802E − 11	ALS vs HC $p = 7.0732E-8$*
	ALS	2.376670	0.016282		PLS vs HC $p = 0.000012$*
	PLS	2.299137	0.028233		ALS vs PLS $p = 0.753316$[a]
Left paracentral gyrus	HC	2.399955	0.015743	0.000008	ALS vs HC $p = 0.006642$*
	ALS	2.330755	0.015718		PLS vs HC $p = 0.000012$*
	PLS	2.250849	0.027254		ALS vs PLS $p = 0.248056$[a]
Right paracentral gyrus	HC	2.390999	0.016011	0.000062	ALS vs HC $p = 0.001250$ *
	ALS	2.309546	0.015986		PLS vs HC $p = 0.000514$*
	PLS	2.268528	0.027718		ALS vs PLS $p = 0.554827$[a]
Left postcentral gyrus	HC	2.030785	0.011406	0.005237	ALS vs HC $p = 0.021473$*
	ALS	1.986822	0.011388		PLS vs HC $p = 1.0$
	PLS	2.047767	0.019746		ALS vs PLS $p = 0.008029$[a]*
Right postcentral gyrus	HC	2.009476	0.011214	0.001836	ALS vs HC $p = 0.023985$*
	ALS	1.966862	0.011196		PLS vs HC $p = 0.598028$
	PLS	2.038370	0.019413		ALS vs PLS $p = 0.030047$[a]*
Left pars triangularis	HC	2.402892	0.016117	0.000297	ALS vs HC $p = 0.000226$*
	ALS	2.310594	0.016091		PLS vs HC $p = 0.097161$
	PLS	2.333436	0.027900		ALS vs PLS $p = 0.098970$[a]
Left pars opercularis	HC	2.524520	0.015812	0.000647	ALS vs HC $p = 0.000874$*
	ALS	2.441884	0.015787		PLS vs HC $p = 0.038135$*
	PLS	2.445018	0.027373		ALS vs PLS $p = 0.138752$[a]

Estimated marginal means and standard error are adjusted for age and gender (age = 59.863, gender = 1.45)

*Significant intergroup differences are flagged with asterisks

[a]The ALS versus PLS post-hoc comparisons are corrected for age, gender and symptom duration. ALS vs HC and PLS vs HC comparisons are corrected for age and gender

they are thought to reflect different aspects of white matter integrity. FA and MD are composite measures of white matter integrity incorporating all three Eigen values. AD alterations are often regarded as a marker of axonal degeneration [55, 56], and RD as an indicator of myelin pathology [57, 58]. However, few histologically validated diffusion imaging studies exist in ALS and PLS and this is likely to be a simplistic interpretation [14]. Reduced primary motor cortex thickness and altered corticospinal tract diffusion metrics have been previously described in PLS compared to healthy controls [59]. The majority of previous PLS studies however have not corrected for symptom duration when comparing PLS and ALS cohorts [12]. In agreement with recent studies [8, 60], corticospinal tract FA and RD were not significantly different between ALS and PLS taking symptom duration into consideration. In this present study we identified significantly reduced post-central gyrus cortical thickness in ALS compared to PLS, but no differences were observed between PLS and controls indicating the sparing of the somatosensory cortex in PLS. A key finding of this present study is the significant cerebellar grey and white matter pathology in PLS compared with ALS, which is not accounted for by symptom duration. One of the rationales to describe distinguishing imaging signatures between MND phenotypes is to aid earlier diagnosis and develop precision prognostic indicators [61–63]. While TDP-43 pathology is a recognised feature of PLS [25, 64], pathological staging systems have not been specifically evaluated in PLS to date [65]. As the post mortem literature of PLS is particularly sparse [6], imaging studies offer unique opportunities to evaluate the distribution of disease burden in vivo [66, 67].

While we have identified widespread cerebellar pathology on imaging, subtle cerebellar signs may be difficult to detect clinically due to co-existing spasticity. It is conceivable that cerebellar dysfunction in PLS contributes to gait impairment, falls and to some extent dysarthria, which are

Table 3 Regional white matter diffusivity values in healthy controls (HC), ALS and PLS

Fractional anisotropy (FA)					
Left corticospinal tract	HC	0.515160	0.002242	4.8482E − 13	ALS vs HC $p = 1.1405E-11$*
	ALS	0.491795	0.002239		PLS vs HC $p = 1.3278E-7$*
	PLS	0.489734	0.003882		ALS vs PLS $p = 0.467469$[a]
Right corticospinal tract	HC	0.523691	0.002492	5.3165E − 11	ALS vs HC $p = 6.1224E-11$*
	ALS	0.498719	0.002488		PLS vs HC $p = 0.000177$*
	PLS	0.503271	0.004314		ALS vs PLS $p = 0.970165$[a]
Left cerebellum	HC	0.382212	0.382212	0.000002	ALS vs HC $p = 0.054100$
	ALS	0.377595	0.001363		PLS vs HC $p = 8.8768E-7$*
	PLS	0.367777	0.002363		ALS vs PLS $p = 0.001126$[a]*
Right cerebellum	HC	0.387413	0.001438	0.000007	ALS vs HC $p = 0.056736$
	ALS	0.382585	0.001436		PLS vs HC $p = 0.000004$*
	PLS	0.373088	0.002489		ALS vs PLS $p = 0.000990$[a]*
Corpus callosum (body)	HC	0.640897	0.003796	1.7196E − 12	ALS vs HC $p = 2.8583E-7$*
	ALS	0.611173	0.003790		PLS vs HC $p = 3.3978E-11$*
	PLS	0.586518	0.006572		ALS vs PLS $p = 0.044785$[a]*
Forceps major	HC	0.724757	0.002499	0.002529	ALS vs HC $p = 0.005861$*
	ALS	0.713636	0.002495		PLS vs HC $p = 0.030813$*
	PLS	0.711810	0.004326		ALS vs PLS $p = 0.246497$[a]
Forceps minor	HC	0.653542	0.003620	0.000246	ALS vs HC $p = 0.000157$*
	ALS	0.632347	0.003614		PLS vs HC $p = 0.926466$
	PLS	0.646150	0.006267		ALS vs PLS $p = 0.315438$[a]
Axial diffusivity (AD)					
Left corticospinal tract	HC	0.001135	0.000003	0.000104	ALS vs HC $p = 0.895070$
	ALS	0.001140	0.000003		PLS vs HC $p = 0.000066$*
	PLS	0.001164	0.000006		ALS vs PLS $p = 0.367058$[a]
Right corticospinal tract	HC	0.001109	0.000004	0.002162	ALS vs HC $p = 0.949760$
	ALS	0.001115	0.000004		PLS vs HC $p = 0.001457$*
	PLS	0.001136	0.000006		ALS vs PLS $p = 0.577055$[a]
Left cerebellum	HC	0.000941	0.000003	0.000005	ALS vs HC $p = 0.890456$
	ALS	0.000937	0.000003		PLS vs HC $p = 0.000094$*
	PLS	0.000966	0.000005		ALS vs PLS $p = 0.073363$[a,t]
Right cerebellum	HC	0.000949	0.000003	0.000444	ALS vs HC $p = 1.0$
	ALS	0.000947	0.000003		PLS vs HC $p = 0.001637$*
	PLS	0.000971	0.000005		ALS vs PLS $p = 0.381128$[a]
Corpus callosum (body)	HC	0.001567	0.000006	0.031909	ALS vs HC $p = 0.037213$*
	ALS	0.001589	0.000006		PLS vs HC $p = 1.0$
	PLS	0.001569	0.000010		ALS vs PLS $p = 0.002532$[a]*
Forceps major	HC	0.001552	0.000006	0.526556	ALS vs HC $p = 1.0$
	ALS	0.001549	0.000006		PLS vs HC $p = 1.0$
	PLS	0.001563	0.000011		ALS vs PLS $p = 0.603960$[a]
Forceps minor	HC	0.001586	0.000008	0.005896	ALS vs HC $p = 0.004135$*
	ALS	0.001624	0.000008		PLS vs HC $p = 0.861954$
	PLS	0.001604	0.000014		ALS vs PLS $p = 0.079298$[a,t]
Radial diffusivity (RD)					
Left corticospinal tract	HC	0.000475	0.000003	3.4456E − 15	ALS vs HC $p = 9.798E-12$*
	ALS	0.000503	0.000003		PLS vs HC $p = 3.8913E-11$*
	PLS	0.000513	0.000005		ALS vs PLS $p = 0.404932$[a]
Right corticospinal tract	HC	0.000453	0.000003	1.786E − 11	ALS vs HC $p = 2.5516E-10$*
	ALS	0.000483	0.000003		PLS vs HC $p = 0.000001$*
	PLS	0.000485	0.000005		ALS vs PLS $p = 0.919832$[a]

Table 3 (continued)

Left cerebellum	HC	0.000509	0.000002	2.3291E − 8	ALS vs HC $p = 0.316724$ PLS vs HC $p = 1.1252E-8$* ALS vs PLS $p = 0.018773$[a]*
	ALS	0.000514	0.000002		
	PLS	0.000537	0.000004		
Right cerebellum	HC	0.000504	0.000002	2.0637E − 8	ALS vs HC $p = 0.291522$ PLS vs HC $p = 9.7631E-9$* ALS vs PLS $p = 0.023847$[a]*
	ALS	0.000509	0.000002		
	PLS	0.000531	0.000004		
Corpus callosum (body)	HC	0.000475	0.000006	3.9569E − 12	ALS vs HC $p = 3.4659E-8$* PLS vs HC $p = 4.9875E-10$* ALS vs PLS $p = 0.497227$[a]
	ALS	0.000525	0.000006		
	PLS	0.000554	0.000010		
Forceps major	HC	0.000363	0.000004	0.013056	ALS vs HC $p = 0.039319$* PLS vs HC $p = 0.051631$t ALS vs PLS $p = 0.246497$[a]
	ALS	0.000377	0.000004		
	PLS	0.000382	0.000007		
Forceps minor	HC	0.000466	0.000007	0.000091	ALS vs HC $p = 0.000057$* PLS vs HC $p = 0.868722$ ALS vs PLS $p = 0.315438$[a]
	ALS	0.000508	0.000007		
	PLS	0.000480	0.000012		

Estimated marginal means and standard error are adjusted for age and gender (Age = 59.863, Gender = 1.45)

*Significant intergroup differences are flagged with asterisks

[a]ALS versus PLS post-hoc comparisons are corrected for age, gender and symptom duration. ALS vs HC and PLS vs HC comparisons are corrected for age and gender

t indicates statistical trends of $0.05 < p < 0.08$

classically attributed to UMN dysfunction alone. Cerebellar dysfunction may not only be masked by UMN signs but is also likely to be under-evaluated on routine clinical assessment. There is also growing evidence that cerebellar pathology may contribute to pseudobulbar affect (pathological crying and laughing) [19, 68–70].

Forty-five PLS patients and the majority of ALS patients underwent genetic testing. Eleven ALS patients detected positive for the *c9orf72* hexanucleotide repeat expansion which may account for some of the extra-motor changes seen in the ALS cohort [71]. Nonetheless, these ALS patients were included in our imaging analyses as their inclusion represents the clinico-genetic heterogeneity of ALS, and this study is primarily aimed at the characterisation of the PLS cohort. While the *C9orf72* repeat expansions have been previously identified in association with PLS [72], no patient in this study tested positive for the *C9orf72* repeat expansion. The genetic risks for PLS are not well established. Suspected PLS patients are often screened for HSP mutations but the co-existing pyramidal and cerebellar degeneration in our PLS cohort raises questions about the rationale to screen for the ever-increasing spectrum SCA genes.

This study is not without limitations. The study has a cross-sectional prospective study design which allows descriptive analyses but the interpretation of dynamic longitudinal changes is not possible [73, 74]. Additional wet biomarker testing, such as the evaluation of neurofilament levels in our cohorts, would have complemented our genetic and imaging analyses [75]. Our findings may shape future research directions, which include robust longitudinal study designs, the recruitment of 'pre-PLS' patients who do not meet diagnostic criteria based on symptom duration and the inclusion of a disease control group with UMN-predominant ALS. The inclusion of pre-PLS patients [15] is particularly important as it would help to establish if imaging analyses can be used to predict risk of conversion to ALS and also to confirm early PLS signatures.

Conclusions

PLS and ALS have both overlapping and distinguishing pathoanatomical signatures, the characterisation of which is relevant to development of diagnostic and prognostic biomarkers. PLS is associated with considerable cerebellar pathology which is difficult to ascertain clinically as it is confounded by concomitant pyramidal degeneration. The extra-motor profile of PLS includes left pars opercularis atrophy which is consistent with the language deficits observed in this cohort. The corpus callosum profile of PLS exhibits selective involvement of the body and splenium. The detailed, multifaceted characterisation of PLS pathology in vivo contributes to the development of phenotype-specific diagnostic protocols, has the potential to shorten the diagnostic journey of individual patients and risk stratification for conversion to ALS. Ultimately, the region of interest analysis of PLS-associated changes in individual patients

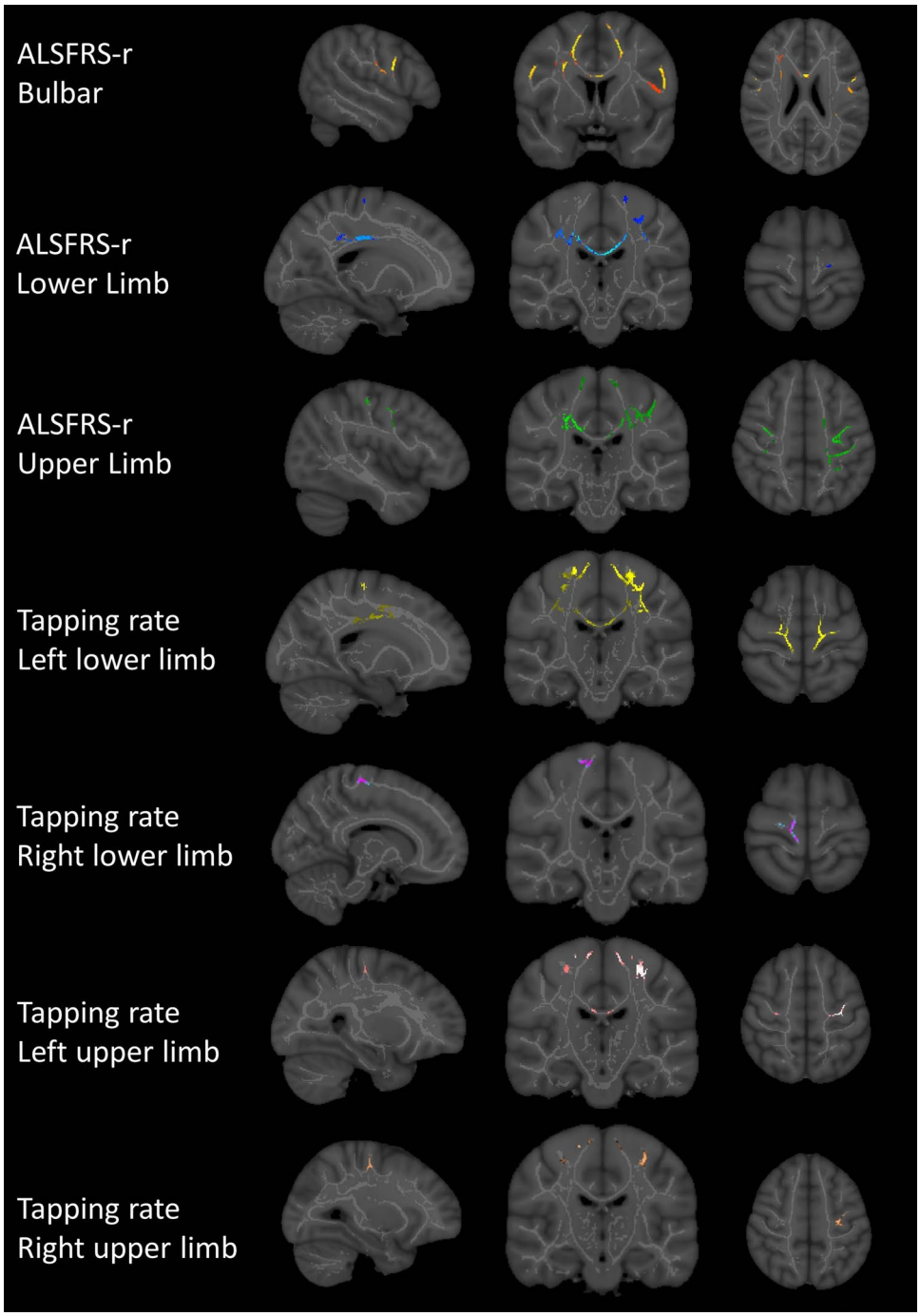

Fig. 5 White matter regions where fractional anisotropy correlates with clinical measures at $p < 0.05$ TFCE FWE adjusting for age and gender. Radiological convention is used

paves the way for the selection of candidate monitoring markers which may be used in future clinical trials.

Acknowledgements The authors are thankful for the kindness and generosity of all patients, their families and the healthy controls for participating in this research project. Without their support, this project would not have been possible. Peter Bede is supported by the Health Research Board (HRB—Ireland; HRB EIA-2017-019), the Andrew Lydon scholarship, the Irish Institute of Clinical Neuroscience IICN—Novartis Ireland Research Grant, the Iris O'Brien Foundation, and the Research Motor Neuron (RMN-Ireland) Foundation. Russell L McLaughlin is supported by the Motor Neurone Disease Association (957-799) and Science Foundation Ireland (17/CDA/4737). Mark A Doherty is supported by Science Foundation Ireland (15/SPP/3244). The sponsors of this study had no role in the design, analyses, presentation of this work or the decision to submit these findings for publication.

Author contributions Drafting the manuscript: EF, PB. Clinical assessments: EF, OH, RHC, CD, NP, PB. Neuroimaging analyses: EF, PB. Genetic analyses: MAD, JCH, AV, RLM. Conceptualisation of the study: EF, OH, PB. Revision of the manuscript for intellectual content: EF, RHC, SLHS, MAD, JCH, AV, CD, RLM, NP, OH, and PB.

Compliance with ethical standards

Conflicts of interest The authors of this manuscript have no conflicts of interest to disclose.

Ethical Standards This study was approved by the Institutional Ethics (Medical Research) Committee, and all participants provided informed consent prior to inclusion.

References

1. Le Forestier N, Maisonobe T, Piquard A, Rivaud S, Crevier-Buchman L, Salachas F, Pradat PF, Lacomblez L, Meininger V (2001) Does primary lateral sclerosis exist? A study of 20 patients and a review of the literature. Brain J Neurol 124(Pt 10):1989–1999
2. Singer MA, Kojan S, Barohn RJ, Herbelin L, Nations SP, Trivedi JR, Jackson CE, Burns DK, Boyer PJ, Wolfe GI (2005) Primary lateral sclerosis: clinical and laboratory features in 25 patients. J Clin Neuromusc Dis 7(1):1–9. https://doi.org/10.1097/01.cnd.0000176974.61136.45
3. Almeida V, de Carvalho M, Scotto M, Pinto S, Pinto A, Ohana B, Swash M (2013) Primary lateral sclerosis: predicting functional outcome. Amyotroph Lateral Scler Frontotemporal Degener 14(2):141–145
4. Gordon PH, Cheng B, Katz IB, Pinto M, Hays AP, Mitsumoto H, Rowland LP (2006) The natural history of primary lateral sclerosis. Neurology 66(5):647–653
5. Floeter MK, Mills R (2009) Progression in primary lateral sclerosis: a prospective analysis. Amyotroph Lateral Sclerosis 10(5–6):339–346
6. Finegan E, Chipika RH, Shing SLH, Hardiman O, Bede P (2019) Primary lateral sclerosis: a distinct entity or part of the ALS spectrum? Amyotroph Lateral Sclerosis Frontotemporal Degener. https://doi.org/10.1080/21678421.2018.1550518
7. Iwata NK, Kwan JY, Danielian LE, Butman JA, Tovar-Moll F, Bayat E, Floeter MK (2011) White matter alterations differ in primary lateral sclerosis and amyotrophic lateral sclerosis. Brain J Neurol 134(9):2642–2655. https://doi.org/10.1093/brain/awr178
8. Müller HP, Gorges M, Kassubek R, Dorst J, Ludolph AC, Kassubek J (2018) Identical patterns of cortico-efferent tract involvement in primary lateral sclerosis and amyotrophic lateral sclerosis: a tract of interest-based MRI study. NeuroImage Clin 18:762–769. https://doi.org/10.1016/j.nicl.2018.03.018
9. Unrath A, Muller H-P, Riecker A, Ludolph AC, Sperfeld A-D, Kassubek J (2010) Whole brain-based analysis of regional white matter tract alterations in rare motor neuron diseases by diffusion tensor imaging. Hum Brain Mapp 31(11):1727–1740
10. Agosta F, Galantucci S, Riva N, Chio A, Messina S, Iannaccone S, Calvo A, Silani V, Copetti M, Falini A, Comi G, Filippi M (2014) Intrahemispheric and interhemispheric structural network abnormalities in PLS and ALS. Hum Brain Mapp 35(4):1710–1722. https://doi.org/10.1002/hbm.22286
11. Butman JA, Floeter MK (2007) Decreased thickness of primary motor cortex in primary lateral sclerosis. Am J Neuroradiol 28(1):87–91
12. Schuster C, Kasper E, Machts J, Bittner D, Kaufmann J, Benecke R, Teipel S, Vielhaber S, Prudlo J (2013) Focal thinning of the motor cortex mirrors clinical features of amyotrophic lateral sclerosis and their phenotypes: a neuroimaging study. J Neurol 260(11):2856–2864
13. Paganoni S, Alshikho MJ, Zürcher NR, Cernasov P, Babu S, Loggia ML, Chan J, Chonde DB, Garcia DI, Catana C, Mainero C, Rosen BR, Cudkowicz ME, Hooker JM, Atassi N (2018) Imaging of glia activation in people with primary lateral sclerosis. NeuroImage Clin 17:347–353. https://doi.org/10.1016/j.nicl.2017.10.024
14. Bede P, Hardiman O (2014) Lessons of ALS imaging: pitfalls and future directions—a critical review. NeuroImage Clin 4:436–443. https://doi.org/10.1016/j.nicl.2014.02.011
15. Clark MG, Smallwood Shoukry R, Huang CJ, Danielian LE, Bageac D, Floeter MK (2018) Loss of functional connectivity is an early imaging marker in primary lateral sclerosis. Amyotroph Lateral Sclerosis Frontotemporal Degener 19(7–8):562–569. https://doi.org/10.1080/21678421.2018.1517180
16. Van Weehaeghe D, Ceccarini J, Delva A, Robberecht W, Van Damme P, Van Laere K (2016) Prospective validation of 18F-FDG brain PET discriminant analysis methods in the diagnosis of amyotrophic lateral sclerosis. J Nucl Med 57(8):1238–1243. https://doi.org/10.2967/jnumed.115.166272
17. Bede P, Bokde A, Elamin M, Byrne S, McLaughlin RL, Jordan N, Hampel H, Gallagher L, Lynch C, Fagan AJ, Pender N, Hardiman O (2013) Grey matter correlates of clinical variables in amyotrophic lateral sclerosis (ALS): a neuroimaging study of ALS motor phenotype heterogeneity and cortical focality. J Neurol Neurosurg Psychiatry 84(7):766–773. https://doi.org/10.1136/jnnp-2012-302674
18. Bede P, Elamin M, Byrne S, Hardiman O (2013) Sexual dimorphism in ALS: exploring gender-specific neuroimaging signatures. Amyotroph Lateral Sclerosis Frontotemporal Degener. https://doi.org/10.3109/21678421.2013.865749
19. Floeter MK, Katipally R, Kim MP, Schanz O, Stephen M, Danielian L, Wu T, Huey ED, Meoded A (2014) Impaired corticopontocerebellar tracts underlie pseudobulbar affect in motor neuron disorders. Neurology 83(7):620–627. https://doi.org/10.1212/wnl.0000000000000693
20. Meoded A, Morrissette AE, Katipally R, Schanz O, Gotts SJ, Floeter MK (2015) Cerebro-cerebellar connectivity is increased in primary lateral sclerosis. NeuroImage Clin 7:288–296
21. Meoded A, Kwan JY, Peters TL, Huey ED, Danielian LE, Wiggs E, Morrissette A, Wu T, Russell JW, Bayat E, Grafman J, Floeter MK (2013) Imaging findings associated with cognitive performance in primary lateral sclerosis and amyotrophic lateral sclerosis. Dementia Geriatr Cognit Disord Extra 3(1):233–250
22. Canu E, Agosta F, Galantucci S, Chio A, Riva N, Silani V, Falini A, Comi G, Filippi M (2013) Extramotor damage is associated with cognition in primary lateral sclerosis patients. PLoS One [Electronic Resource] 8(12):e82017
23. Tu S, Menke RAL, Talbot K, Kiernan MC, Turner MR (2019) Cerebellar tract alterations in PLS and ALS. Amyotroph Lateral Sclerosis Frontotemporal Degener 20(3–4):281–284. https://doi.org/10.1080/21678421.2018.1562554
24. Bede P, Querin G, Pradat PF (2018) The changing landscape of motor neuron disease imaging: the transition from descriptive studies to precision clinical tools. Curr Opin Neurol 31(4):431–438. https://doi.org/10.1097/wco.0000000000000569
25. Dickson DW, Josephs KA, Amador-Ortiz C (2007) TDP-43 in differential diagnosis of motor neuron disorders. Acta Neuropathol 114(1):71–79
26. Kosaka T, Fu YJ, Shiga A, Ishidaira H, Tan CF, Tani T, Koike R, Onodera O, Nishizawa M, Kakita A, Takahashi H (2012) Primary lateral sclerosis: upper-motor-predominant amyotrophic lateral sclerosis with frontotemporal lobar degeneration–immunohistochemical and biochemical analyses of TDP-43. Neuropathol Off J Japan Society Neuropathol 32(4):373–384
27. Brooks BR, Miller RG, Swash M, Munsat TL, World Federation of Neurology Research Group on Motor Neuron D (2000) El Escorial revisited: revised criteria for the diagnosis of amyotrophic lateral sclerosis. Amyotroph Lateral Sclerosis Other Motor

Neuron Disord Off Publ World Feder Neurol Res Group Motor Neuron Dis 1(5):293–299
28. Woo JH, Wang S, Melhem ER, Gee JC, Cucchiara A, McCluskey L, Elman L (2014) Linear associations between clinically assessed upper motor neuron disease and diffusion tensor imaging metrics in amyotrophic lateral sclerosis. PLoS One [Electronic Resource] 9(8):e105753
29. Bohannon RW, Smith MB (1987) Interrater reliability of a modified Ashworth scale of muscle spasticity. Phys Ther 67(2):206–207
30. Pinto-Grau M, Burke T, Lonergan K, McHugh C, Mays I, Madden C, Vajda A, Heverin M, Elamin M, Hardiman O, Pender N (2017) Screening for cognitive dysfunction in ALS: validation of the Edinburgh Cognitive and Behavioural ALS Screen (ECAS) using age and education adjusted normative data. Amyotroph Lateral Sclerosis Frontotemporal Degener 18(1–2):99–106. https://doi.org/10.1080/21678421.2016.1249887
31. Cedarbaum JM, Stambler N, Malta E, Fuller C, Hilt D, Thurmond B, Nakanishi A (1999) The ALSFRS-R: a revised ALS functional rating scale that incorporates assessments of respiratory function. BDNF ALS Study Group (Phase III). J Neurol Sci 169(1–2):13–21
32. Martin M (2011) Cutadapt removes adapter sequences from high-throughput sequencing reads. EMBnetjournal 17:10–12
33. Li H, Handsaker B, Wysoker A, Fennell T, Ruan J, Homer N, Marth G, Abecasis G, Durbin R, Genome Project Data Processing S (2009) The sequence alignment/map format and SAMtools. Bioinformatics (Oxford, England) 25(16):2078–2079. https://doi.org/10.1093/bioinformatics/btp352
34. Purcell S, Neale B, Todd-Brown K, Thomas L, Ferreira MAR, Bender D, Maller J, Sklar P, de Bakker PIW, Daly MJ, Sham PC (2007) PLINK: a tool set for whole-genome association and population-based linkage analyses. Am J Hum Genet 81(3):559–575. https://doi.org/10.1086/519795
35. Cingolani P, Platts A, Wang LL, Coon M, Nguyen T, Wang L, Land SJ, Lu X, Ruden DM (2012) A program for annotating and predicting the effects of single nucleotide polymorphisms, SnpEff: SNPs in the genome of *Drosophila melanogaster* strain w1118; iso-2; iso-3. Fly 6(2):80–92. https://doi.org/10.4161/fly.19695
36. Paila U, Chapman BA, Kirchner R, Quinlan AR (2013) GEMINI: integrative exploration of genetic variation and genome annotations. PLoS Comput Biol 9(7):e1003153. https://doi.org/10.1371/journal.pcbi.1003153
37. Project Min EALSSC (2018) Project MinE: study design and pilot analyses of a large-scale whole-genome sequencing study in amyotrophic lateral sclerosis. Eur J Hum Genet EJHG 26(10):1537–1546. https://doi.org/10.1038/s41431-018-0177-4
38. Abel O, Shatunov A, Jones AR, Andersen PM, Powell JF, Al-Chalabi A (2013) Development of a smartphone app for a genetics website: the amyotrophic lateral sclerosis online genetics database (ALSoD). JMIR mHealth uHealth 1(2):e18–e18. https://doi.org/10.2196/mhealth.2706
39. Klebe S, Stevanin G, Depienne C (2015) Clinical and genetic heterogeneity in hereditary spastic paraplegias: from SPG1 to SPG72 and still counting. Rev Neurol (Paris) 171(6–7):505–530. https://doi.org/10.1016/j.neurol.2015.02.017
40. Lek M, Karczewski KJ, Minikel EV, Samocha KE, Banks E, Fennell T, O'Donnell-Luria AH, Ware JS, Hill AJ, Cummings BB, Tukiainen T, Birnbaum DP, Kosmicki JA, Duncan LE, Estrada K, Zhao F, Zou J, Pierce-Hoffman E, Berghout J, Cooper DN, Deflaux N, DePristo M, Do R, Flannick J, Fromer M, Gauthier L, Goldstein J, Gupta N, Howrigan D, Kiezun A, Kurki MI, Moonshine AL, Natarajan P, Orozco L, Peloso GM, Poplin R, Rivas MA, Ruano-Rubio V, Rose SA, Ruderfer DM, Shakir K, Stenson PD, Stevens C, Thomas BP, Tiao G, Tusie-Luna MT, Weisburd B, Won HH, Yu D, Altshuler DM, Ardissino D, Boehnke M, Danesh J, Donnelly S, Elosua R, Florez JC, Gabriel SB, Getz G, Glatt SJ, Hultman CM, Kathiresan S, Laakso M, McCarroll S, McCarthy MI, McGovern D, McPherson R, Neale BM, Palotie A, Purcell SM, Saleheen D, Scharf JM, Sklar P, Sullivan PF, Tuomilehto J, Tsuang MT, Watkins HC, Wilson JG, Daly MJ, MacArthur DG (2016) Analysis of protein-coding genetic variation in 60,706 humans. Nature 536(7616):285–291. https://doi.org/10.1038/nature19057
41. Auton A, Brooks LD, Durbin RM, Garrison EP, Kang HM, Korbel JO, Marchini JL, McCarthy S, McVean GA, Abecasis GR (2015) A global reference for human genetic variation. Nature 526(7571):68–74. https://doi.org/10.1038/nature15393
42. Stenson PD, Mort M, Ball EV, Evans K, Hayden M, Heywood S, Hussain M, Phillips AD, Cooper DN (2017) The Human Gene Mutation Database: towards a comprehensive repository of inherited mutation data for medical research, genetic diagnosis and next-generation sequencing studies. Hum Genet 136(6):665–677. https://doi.org/10.1007/s00439-017-1779-6
43. Byrne S, Elamin M, Bede P, Shatunov A, Walsh C, Corr B, Heverin M, Jordan N, Kenna K, Lynch C, McLaughlin RL, Iyer PM, O'Brien C, Phukan J, Wynne B, Bokde AL, Bradley DG, Pender N, Al-Chalabi A, Hardiman O (2012) Cognitive and clinical characteristics of patients with amyotrophic lateral sclerosis carrying a C9orf72 repeat expansion: a population-based cohort study. Lancet Neurol 11(3):232–240. https://doi.org/10.1016/S1474-4422(12)70014-5
44. Kenna KP, McLaughlin RL, Byrne S, Elamin M, Heverin M, Kenny EM, Cormican P, Morris DW, Donaghy CG, Bradley DG, Hardiman O (2013) Delineating the genetic heterogeneity of ALS using targeted high-throughput sequencing. J Med Genet 50(11):776–783. https://doi.org/10.1136/jmedgenet-2013-101795
45. Douaud G, Smith S, Jenkinson M, Behrens T, Johansen-Berg H, Vickers J, James S, Voets N, Watkins K, Matthews PM, James A (2007) Anatomically related grey and white matter abnormalities in adolescent-onset schizophrenia. Brain J Neurol 130(Pt 9):2375–2386
46. Good CD, Johnsrude IS, Ashburner J, Henson RN, Friston KJ, Frackowiak RS (2001) A voxel-based morphometric study of ageing in 465 normal adult human brains. NeuroImage 14(1 Pt 1):21–36
47. Fischl B (2012) FreeSurfer. NeuroImage 62(2):774–781. https://doi.org/10.1016/j.neuroimage.2012.01.021
48. Fischl B, Dale AM (2000) Measuring the thickness of the human cerebral cortex from magnetic resonance images. Proc Natl Acad Sci 97(20):11050–11055. https://doi.org/10.1073/pnas.200033797
49. Desikan RS, Segonne F, Fischl B, Quinn BT, Dickerson BC, Blacker D, Buckner RL, Dale AM, Maguire RP, Hyman BT, Albert MS, Killiany RJ (2006) An automated labeling system for subdividing the human cerebral cortex on MRI scans into gyral based regions of interest. NeuroImage 31(3):968–980. https://doi.org/10.1016/j.neuroimage.2006.01.021
50. Wakana S, Caprihan A, Panzenboeck MM, Fallon JH, Perry M, Gollub RL, Hua K, Zhang J, Jiang H, Dubey P, Blitz A, van Zijl P, Mori S (2007) Reproducibility of quantitative tractography methods applied to cerebral white matter. NeuroImage 36(3):630–644. https://doi.org/10.1016/j.neuroimage.2007.02.049
51. Bede P, Elamin M, Byrne S, McLaughlin RL, Kenna K, Vajda A, Fagan A, Bradley DG, Hardiman O (2015) Patterns of cerebral and cerebellar white matter degeneration in ALS. J Neurol Neurosurg Psychiatry 86(4):468–470. https://doi.org/10.1136/jnnp-2014-308172
52. Schuster C, Elamin M, Hardiman O, Bede P (2016) The segmental diffusivity profile of amyotrophic lateral sclerosis associated white matter degeneration. Eur J Neurol 23(8):1361–1371. https://doi.org/10.1111/ene.13038

53. Bersano E, Sarnelli MF, Solara V, De Marchi F, Sacchetti GM, Stecco A, Corrado L, D'Alfonso S, Cantello R, Mazzini L (2018) A case of late-onset OCD developing PLS and FTD. Amyotroph Lateral Sclerosis Frontotemporal Degener 19(5–6):463–465. https://doi.org/10.1080/21678421.2018.1440405
54. de Vries BS, Rustemeijer LMM, van der Kooi AJ, Raaphorst J, Schröder CD, Nijboer TCW, Hendrikse J, Veldink JH, van den Berg LH, van Es MA (2017) A case series of PLS patients with frontotemporal dementia and overview of the literature. Amyotroph Lateral Sclerosis Frontotemporal Degener 18(7–8):534–548. https://doi.org/10.1080/21678421.2017.1354996
55. Budde MD, Xie M, Cross AH, Song SK (2009) Axial diffusivity is the primary correlate of axonal injury in the experimental autoimmune encephalomyelitis spinal cord: a quantitative pixelwise analysis. J Neurosci Off J Soc Neurosci 29(9):2805–2813. https://doi.org/10.1523/JNEUROSCI.4605-08.2009
56. Sun SW, Liang HF, Trinkaus K, Cross AH, Armstrong RC, Song SK (2006) Noninvasive detection of cuprizone induced axonal damage and demyelination in the mouse corpus callosum. Magn Reson Med Off J Soc Magn Reson Med Soc Magn Reson Med 55(2):302–308. https://doi.org/10.1002/mrm.20774
57. Song SK, Sun SW, Ramsbottom MJ, Chang C, Russell J, Cross AH (2002) Dysmyelination revealed through MRI as increased radial (but unchanged axial) diffusion of water. NeuroImage 17(3):1429–1436
58. Song SK, Yoshino J, Le TQ, Lin SJ, Sun SW, Cross AH, Armstrong RC (2005) Demyelination increases radial diffusivity in corpus callosum of mouse brain. NeuroImage 26(1):132–140. https://doi.org/10.1016/j.neuroimage.2005.01.028
59. Ulug AM, Grunewald T, Lin MT, Kamal AK, Filippi CG, Zimmerman RD, Beal MF (2004) Diffusion tensor imaging in the diagnosis of primary lateral sclerosis. J Magn Reson Imaging 19(1):34–39
60. Muller HP, Agosta F, Riva N, Spinelli EG, Comi G, Ludolph AC, Filippi M, Kassubek J (2018) Fast progressive lower motor neuron disease is an ALS variant: a two-centre tract of interest-based MRI data analysis. NeuroImage Clin 17:145–152. https://doi.org/10.1016/j.nicl.2017.10.008
61. Schuster C, Hardiman O, Bede P (2017) Survival prediction in amyotrophic lateral sclerosis based on MRI measures and clinical characteristics. BMC Neurol 17(1):73. https://doi.org/10.1186/s12883-017-0854-x
62. Schuster C, Hardiman O, Bede P (2016) Development of an automated MRI-based diagnostic protocol for amyotrophic lateral sclerosis using disease-specific pathognomonic features: a quantitative disease-state classification study. PLoS ONE 11(12):e0167331. https://doi.org/10.1371/journal.pone.0167331
63. Grollemund V, Pradat PF, Querin G, Delbot F, Le Chat G, Pradat-Peyre JF, Bede P (2019) Machine learning in amyotrophic lateral sclerosis: achievements, pitfalls, and future directions. Front Neurosci 13:135. https://doi.org/10.3389/fnins.2019.00135
64. Dickson DW (2008) TDP-43 immunoreactivity in neurodegenerative disorders: disease versus mechanism specificity. Acta Neuropathol 115(1):147–149. https://doi.org/10.1007/s00401-007-0323-5
65. Brettschneider J, Del Tredici K, Toledo JB, Robinson JL, Irwin DJ, Grossman M, Suh E, Van Deerlin VM, Wood EM, Baek Y, Kwong L, Lee EB, Elman L, McCluskey L, Fang L, Feldengut S, Ludolph AC, Lee VM, Braak H, Trojanowski JQ (2013) Stages of pTDP-43 pathology in amyotrophic lateral sclerosis. Ann Neurol 74(1):20–38. https://doi.org/10.1002/ana.23937
66. Bede P, Hardiman O (2014) Lessons of ALS imaging: pitfalls and future directions—a critical review. NeuroImage Clin 4:436–443. https://doi.org/10.1016/j.nicl.2014.02.011
67. Turner MR, Agosta F, Bede P, Govind V, Lule D, Verstraete E (2012) Neuroimaging in amyotrophic lateral sclerosis. Biomark Med 6(3):319–337. https://doi.org/10.2217/bmm.12.26
68. Christidi F, Karavasilis E, Ferentinos P, Xirou S, Velonakis G, Rentzos M, Zouvelou V, Zalonis I, Efstathopoulos E, Kelekis N, Evdokimidis I (2018) Investigating the neuroanatomical substrate of pathological laughing and crying in amyotrophic lateral sclerosis with multimodal neuroimaging techniques. Amyotroph Lateral Sclerosis Frontotemporal Degener 19(1–2):12–20. https://doi.org/10.1080/21678421.2017.1386689
69. Stoodley CJ, Schmahmann JD (2010) Evidence for topographic organization in the cerebellum of motor control versus cognitive and affective processing. Cortex 46(7):831–844. https://doi.org/10.1016/j.cortex.2009.11.008
70. Bede P, Finegan E (2018) Revisiting the pathoanatomy of pseudobulbar affect: mechanisms beyond corticobulbar dysfunction. Amyotroph Lateral Sclerosis Frontotemporal Degener 19(1–2):4–6. https://doi.org/10.1080/21678421.2017.1392578
71. Bede P, Bokde ALW, Byrne S, Elamin M, McLaughlin RL, Kenna K, Fagan AJ, Pender N, Bradley DG, Hardiman O (2013) Multiparametric MRI study of ALS stratified for the C9orf72 genotype. Neurology 81(4):361–369. https://doi.org/10.1212/WNL.0b013e31829c5eee
72. Mitsumoto H, Nagy PL, Gennings C, Murphy J, Andrews H, Goetz R, Floeter MK, Hupf J, Singleton J, Barohn RJ, Nations S, Shoesmith C, Kasarskis E, Factor-Litvak P (2015) Phenotypic and molecular analyses of primary lateral sclerosis. Neurol Genet. https://doi.org/10.1212/01.NXG.0000464294.88607.dd
73. Chipika RH, Finegan E, Li Hi Shing S, Hardiman O, Bede P (2019) tracking a fast-moving disease: longitudinal markers, monitoring, and clinical trial endpoints in ALS. Front Neurol 10:229. https://doi.org/10.3389/fneur.2019.00229
74. Schuster C, Elamin M, Hardiman O, Bede P (2015) Presymptomatic and longitudinal neuroimaging in neurodegeneration–from snapshots to motion picture: a systematic review. J Neurol Neurosurg Psychiatry 86(10):1089–1096. https://doi.org/10.1136/jnnp-2014-309888
75. Steinacker P, Feneberg E, Weishaupt J, Brettschneider J, Tumani H, Andersen PM, von Arnim CA, Bohm S, Kassubek J, Kubisch C, Lule D, Muller HP, Muche R, Pinkhardt E, Oeckl P, Rosenbohm A, Anderl-Straub S, Volk AE, Weydt P, Ludolph AC, Otto M (2016) Neurofilaments in the diagnosis of motoneuron diseases: a prospective study on 455 patients. J Neurol Neurosurg Psychiatry 87(1):12–20. https://doi.org/10.1136/jnnp-2015-311387